Proc. Natl. Acad. Sci. USA
Vol. 90, pp. 8619–8623, September 1993
Biochemistry

Kinetic characterization of a cytoplasmic myosin motor domain expressed in *Dictyostelium discoideum*

MARCIA D. RITCHIE*, MICHAEL A. GEEVES*, SALLY K. A. WOODWARD†, AND DIETMAR J. MANSTEIN†

*Department of Biochemistry, School of Medical Sciences, University of Bristol, University Walk, Bristol, BS8 1TD, United Kingdom; and †National Institute for Medical Research, The Ridgeway, Mill Hill, London, NW7 1AA, United Kingdom

Communicated by James A. Spudich, June 24, 1993

ABSTRACT **A detailed kinetic study of the interaction of a recombinant myosin head fragment (MHF) of *Dictyostelium discoideum* with actin and adenine nucleotides has been made by using a combination of rapid-reaction, equilibrium, and fluorescence methods. MHF is equivalent in size to a proteolytic fragment of skeletal muscle myosin, subfragment 1 (S1), the simplest unit of myosin to retain enzymatic and functional activity. The results show that qualitatively the interactions of MHF with nucleotides and actin are the same as those of S1. Both bind to rabbit actin with the same affinity, although differences in the rate constants of their interactions with nucleotides in the presence and absence of actin occur. The rate of ATP binding to MHF and the subsequent cleavage step are significantly slower than the corresponding rates with S1. The dissociation of a fluorescent analog of ADP from MHF was 5-fold faster than from S1, while its rate of binding MHF was 3-fold slower, resulting in a weaker association equilibrium constant. The ATP-induced isomerization of the actoMHF complex was 10-fold slower than for actoS1, but the binding affinities of ADP for actoMHF and actoS1 were indistinguishable. The results suggest a different degree of coupling between the nucleotide and actin binding sites of MHF and S1 which may be a common feature of nonmuscle myosins. They also provide the basis for a study of specifically modified myosins with which one can probe the sites of interaction with nucleotides or actin, as well as functional motility.**

Conventional myosins of the filament-forming type occur in nearly every eukaryotic cell examined. Their interaction with actin filaments underlies a variety of motile activities including muscle contraction, capping of cell surface receptors, and cytokinesis. The energy required to generate force and displacement in these interactions is provided by ATP. Molecular studies of protein structure and enzymatic activity are necessary in order to understand the mechanism by which myosin catalyzes this transduction of energy. In particular, kinetic measurements can be used to determine the rate and equilibrium constants that define the mechanism of ATP hydrolysis and constrain thermodynamic models of energy transduction. Myosins isolated from striated, smooth, and cardiac muscle have been well characterized in kinetic terms (1, 2). In contrast, much less is known about nonmuscle or cytoplasmic myosins. The kinetic characterization of cytoplasmic myosins has been restricted both by their lower tissue abundance and by the difficulty of generating soluble proteolytic fragments incorporating a functional motor domain.

In this study, we describe the kinetic characterization of a recombinant motor domain derived from a cytoplasmic myosin. This myosin head fragment (MHF) was expressed in the motile eukaryotic organism *Dictyostelium discoideum*. MHF is the product of a translational fusion of the eighth codon of the *Dictyostelium act-15* gene to the second codon of the *Dictyostelium mhcA* gene (3). The polypeptide encoded by this fusion has 871 amino acids and resembles subfragment 1 (S1), the simplest functional myosin fragment known to retain all the enzymatic properties of myosin (4). The interactions of MHF with rabbit skeletal muscle actin and nucleotide are described and compared with those of rabbit S1. Using equilibrium and kinetic binding methods, we have shown that S1 and MHF bind with the same affinity to actin. Further, the interaction of nucleotide with MHF, both in the presence and in the absence of actin, follows the same mechanism as S1, but many of the steps are significantly slower.

MATERIALS AND METHODS

Proteins and Reagents. *Dictyostelium* MHF was purified from frozen stocks of cell line HS2210 (3). Cells were grown in a 50-liter fermenter and harvested at a density of 3.5×10^6 cells per milliliter using a Millipore Prostak filtration device fitted with a 10-square-foot, 0.6-μm membrane, with a circulation rate of 12 liters/min. To initiate development, cells were suspended in starvation buffer (20 mM Mes, pH 6.9/0.2 mM $CaCl_2$/2 mM $MgCl_2$/125 mM sucrose) and shaken on a gyratory shaker at 140 rpm for 3.5 hr. The developed cells were washed with TE buffer (10 mM Tris·HCl, pH 8.0/1 mM EDTA) and suspended in 1 ml of lysis buffer per gram of cells [50 mM Hepes·KOH, pH 7.5/100 mM KCl/2 mM EDTA/0.2 mM EGTA/1 mM dithiothreitol/5 mM benzamidine/30% (wt/vol) sucrose containing "tosyl-lysine chloromethyl ketone" (7-amino-1-chloro-3-tosylamido-2-heptanone, 40 μg/ml) and leupeptin (10 μg/ml)]. This suspension was slowly pipetted into liquid nitrogen and the resulting pellets were stored at −80°C in aliquots corresponding to ≈100 g of cells. Cell lysis took place upon thawing of these pellets. MHF was purified as described (3) and on elution from the final Superose 12 column was concentrated to ≈25 mg/ml (Centricon 30, Amicon). After addition of sucrose to 30% (wt/vol), the protein was stored at −80°C. MHF stored in this way was stable for at least 1 year and displayed no loss of activity within this period, even after repeated thawing and freezing.

Dictyostelium myosin was purified by the method of Uyeda and Ruppel (5) and rabbit myosin by the method of Margossian and Lowey (6). Rabbit S1 was prepared by chymotryptic digestion of rabbit myosin (7). F-actin was isolated as described (8). The preparation of pyrene-labeled actin (pyr-actin) has been described (9). Molar concentrations were determined at 280 nm by using the following extinction coefficients: $\varepsilon_{280}^{1\%} = 7.9$ cm^{-1} and a molecular weight of 115,000 for S1 (5); $\varepsilon_{280}^{1\%} = 11.08$ cm^{-1} and a molecular weight of 42,000 for actin (10). In determining the concentration of pyr-actin, a correction was first made for the absorbance of the label at 280 nm (A_{280} pyrene = 1.06 × A_{344}) (9). The

The publication costs of this article were defrayed in part by page charge payment. This article must therefore be hereby marked "*advertisement*" in accordance with 18 U.S.C. §1734 solely to indicate this fact.

Abbreviations: MHF, myosin head fragment; S1, subfragment 1; pyr-actin, pyrene-labeled actin; mantADP, 2′(3′)-*O*-(*N*-methylanthraniloyl)adenosine 5′-diphosphate.

concentration of MHF was determined at 280 nm by using $\varepsilon_{280}^{1\%} = 8.0\ cm^{-1}$ and a molecular weight of 130,000.

N-Methylanthraniloyl derivatives of ATP and ADP (mantATP and mantADP), prepared and characterized by the method of Hiratsuka (11), were a kind gift of J. F. Eccleston (National Institute of Medical Research, London). All other reagents were of analytical grade and were used without further purification.

Stopped-Flow Experiments and Fluorescence Titrations. Stopped-flow experiments were performed at 20°C with a Hi-tech Scientific SF-51 stopped-flow spectrophotometer. Light was provided by a Hammamatsu 100-W Xe/Hg lamp and passed through a Photon Technology International LP S-20 monochromator. Reactions were followed by measurement of pyrene fluorescence excited at 365 nm and monitored at 90° through a KV 389-nm-cutoff filter. Data were captured on a Das-50 analog/digital board, stored as 500 points per data set, and analyzed by a least-squares fitting procedure on a Viglen 386 computer using software provided by Hi-Tech. All transients shown are the average of three to five consecutive data sets. All concentrations refer to the concentration of the reactants after mixing in the stopped-flow cell.

Fluorescence titrations were carried out on a Perkin–Elmer LS 5B Luminescence Spectrophotometer at 20°C, using excitation/emission bandwidths of 2.5 nm. Typical working volumes of 600 μl were used.

RESULTS

Fluorescence Titrations. The binding of S1 to pyr-actin results in a 60–70% quenching of the pyrene fluorescence (12, 13) and provides a monitor of this interaction. A titration of 0.5 μM pyr-actin with MHF at low ionic strength (30 mM) shows that MHF binds to pyr-actin and quenches the fluorescence by 80%, somewhat greater quenching than that observed for rabbit skeletal S1. Under the conditions of this titration the concentration of pyr-actin is much greater than the equilibrium dissociation constant, and saturation of the actin occurs at stoichiometric MHF concentration. This allowed the concentration of actin binding sites to be estimated as 25 μM for MHF, a value in good agreement with that estimated by using the extinction coefficient at 280 nm (28 μM).

A similar titration using concentrations of pyr-actin close to its dissociation constant for binding S1 allowed this constant to be measured accurately for MHF. This is possible for S1 at ionic strengths of >0.1 M, where the dissociation constant is greater than 0.05 μM. In Fig. 1 titrations at elevated ionic strength are shown for S1 and MHF, using pyr-actin at 0.6 μM. The dissociation constant was determined as described (13) and values of 0.07 μM for both rabbit S1 and *Dictyostelium* MHF were obtained. The affinity of *Dictyostelium* MHF for actin is indistinguishable from that of rabbit S1 under the conditions used.

Binding of ATP to ActoS1 and ActoMHF Complexes. The binding of ATP to pyr-actoS1 results in dissociation of the complex. The progress of this reaction was followed by measurement of the resulting increase in pyrene fluorescence as dissociation occurred, shown in Fig. 2*A* for the actoMHF complex. The rate of the observed single exponential was linearly dependent on ATP concentration from 5 to 25 μM ATP (Fig. 2*B*). The slope of this plot defines the second-order rate constant $K_a \cdot k_b$ (see Scheme I). For actoS1 this was $1.8 \times 10^6\ M^{-1} \cdot s^{-1}$, while for actoMHF it was $0.15 \times 10^6\ M^{-1} \cdot s^{-1}$, ≈12-fold slower. To determine whether this slower rate of ATP binding is a property of the native myosins, the above experiment was repeated with actomyosin. The second-order rate constants obtained were $4.7 \times 10^5\ M^{-1} \cdot s^{-1}$ and $0.3 \times 10^5\ M^{-1} \cdot s^{-1}$ for rabbit and *Dictyostelium* actomyosin, respectively (Fig. 2*C*). The reduction in absolute rates observed for both proteins is a consequence of the increased salt concentration (0.5 M KCl) used to solubilize the proteins. However, the ratio of the rate constants for rabbit and *Dictyostelium* myosins is close to that observed for the soluble fragments.

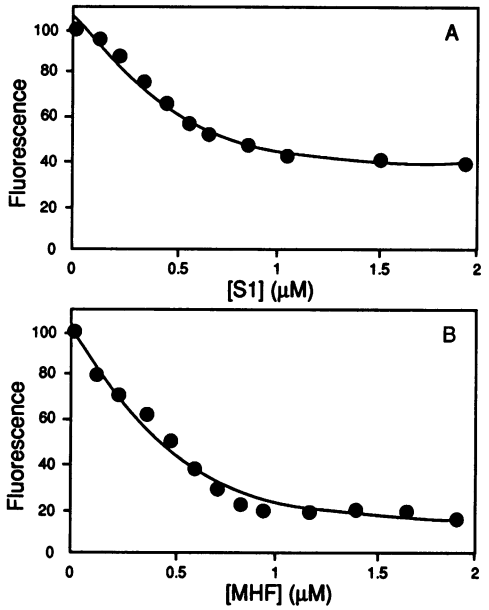

FIG. 1. Fluorescence titration of pyr-actin with myosin subfragments. Pyrene fluorescence excited at 365 nm and monitored at 407 nm was measured. (*A*) Titration of 0.6 μM pyr-actin with rabbit S1. K_d = 0.07 μM. (*B*) Titration of 0.5 μM pyr-actin with *Dictyostelium* MHF. K_d = 0.07 μM. Conditions: 25 mM Hepes, 100 mM KCl, 5 mM $MgCl_2$, pH 7.0, 20°C. Phalloidin (0.5 μM) was used to stabilize F-actin.

At 20°C, the observed rate of ATP-induced dissociation of actoS1 is linearly dependent on ATP concentration, although at concentrations of ATP above 200 μM this rate becomes too fast to measure in the stopped-flow apparatus. However, at 1°C the reaction is slowed sufficiently so that higher ATP concentrations may be used. At this temperature the observed rate has an approximately hyperbolic dependence on ATP concentration, with a maximum of 500 s^{-1}. Slow and smooth muscle myosins show the same hyperbolic ATP concentration dependence at ambient temperatures (14, 15). This relationship has been analyzed in terms of the following model:

$$A \cdot M + ATP \overset{K_a}{\rightleftharpoons} A \cdot M \cdot ATP \overset{k_b}{\rightarrow} A + M \cdot ATP,$$

Scheme I

where A and M represent actin and myosin. The first step is a rapid equilibrium, defined by the equilibrium constant K_a, and the second step a protein isomerization preceding actin dissociation, with a rate constant, k_b. For this model (16),

$$k_{obs} = K_a \cdot k_b \cdot [ATP]/(1 + K_a \cdot [ATP]).$$

The concentration dependence of the ATP-induced dissociation of pyr-actoMHF at 20°C, from 0 to 15 mM ATP, is shown in Fig. 2*D*; a hyperbolic dependence was observed, with K_a = 320 M^{-1} and k_b = 450 s^{-1}. Under the same conditions, fast rabbit S1 is predicted to give K_a = 500 M^{-1} and k_b = 5000 s^{-1}. Thus k_b is reduced ≈10-fold, whereas K_a is not greatly affected. The product, $K_a \cdot k_b$, gives a value of $0.14 \times 10^6\ M^{-1} \cdot s^{-1}$ for the second-order rate constant of ATP binding to *Dictyostelium* actoMHF and is in agreement with the data shown in Fig. 2*B*.

Binding of ADP to ActoS1 and ActoMHF Complexes. The affinity of ADP for actoS1 and actoMHF was determined by

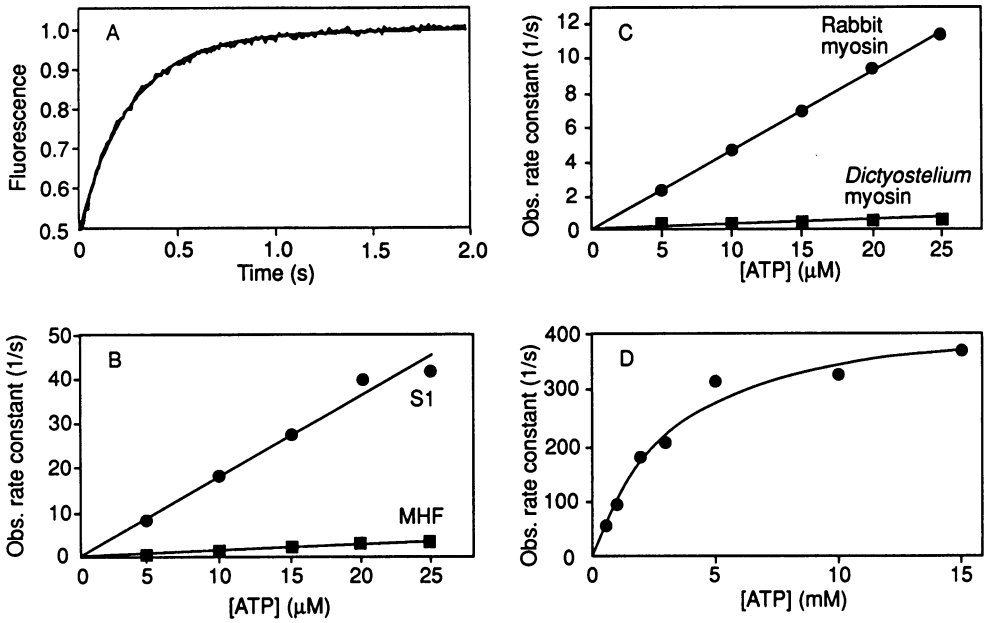

FIG. 2. ATP-induced dissociation of actoS1 and actoMHF complexes. (*A*) Stopped-flow record observed on mixing 0.25 μM actoMHF with 25 μM ATP. Pyrene fluorescence excited at 365 nm was monitored. The solid line is the best fit to a single exponential. $k_{obs} = 2.51\ s^{-1}$. (*B*) Dependence of the rate of the observed processes on ATP concentration for rabbit S1 and *Dictyostelium* MHF. The solid line is the best fit to a straight line. $K_a \cdot k_{+b} = 1.8 \times 10^6\ M^{-1} s^{-1}$ for rabbit S1 and $0.15 \times 10^6\ M^{-1} s^{-1}$ for *Dictyostelium* MHF. Conditions: 25 mM Hepes, 0.1 M KCl, 5 mM $MgCl_2$, pH 7.0, 20°C. (*C*) As in *B*; myosin replaces MHF and S1. $K_a \cdot k_{+b}$ values of $4.7 \times 10^5\ M^{-1} s^{-1}$ (rabbit myosin) and $0.3 \times 10^5\ M^{-1} s^{-1}$ (*Dictyostelium* myosin) were determined. Conditions: 25 mM Hepes, 0.5 M KCl, 5 mM $MgCl_2$, pH 7.0, 20°C. (*D*) Determination of the maximum rate of ATP binding to actoMHF. ActoMHF (0.5 μM) was mixed with ATP in the stopped-flow apparatus. $K_a = 320\ M^{-1}$, $k_b = 450\ s^{-1}$. Conditions were as described for *B*.

measurement of the competitive inhibition by ADP of the ATP-induced dissociation of the actoS1 or actoMHF complex. A reduction in the observed rate occurs as ADP concentration is increased at constant ATP concentration. Under conditions where ADP binding is rapid compared with the rate of ATP-induced dissociation, the following model (17) applies:

$$A{\cdot}M{\cdot}ADP \overset{K_{AD}}{\rightleftharpoons} A{\cdot}M + ATP \overset{k_0}{\rightarrow} A + M{\cdot}ATP$$
$$k_{obs} = k_0/(1 + [ADP]{\cdot}K_{AD}),$$

Scheme II

where k_0 is the observed rate constant in the absence of ADP, and K_{AD} is the equilibrium dissociation constant of ADP for the actoS1 or actoMHF complex. The best fit of our experimental data to the above equation gave similar K_{AD} values for actoS1 ($8.55 \times 10^3\ M^{-1}$) and actoMHF ($10.6 \times 10^3\ M^{-1}$).

The equilibrium binding of pyr-actin to S1 and MHF in the presence of ADP was determined by fluorescence titration. S1 or MHF was added to 0.5 μM pyr-actin and 2 mM ADP. The titration yielded association rate constants of $1 \times 10^6\ M^{-1}$ and $5 \times 10^6\ M^{-1}$ for S1 and MHF, respectively (see K_{DA} in Table 2).

Interaction of Nucleotides with S1 and MHF. The binding of ATP to S1 and MHF in the absence of actin was followed by measurement of the resulting enhancement of intrinsic protein fluorescence (18–20). At 20°C, these data are described by a single exponential (Fig. 3*A*). The fluorescence change observed upon ATP binding to MHF was 50% that of S1. The dependence of the rate of the observed processes on ATP concentration was approximately hyperbolic (Fig. 3*B*). The maximal rate, k_{max}, observed for MHF ($24.3\ s^{-1}$) was ≈5 times slower than that for S1 ($131\ s^{-1}$). For S1 this maximal rate of fluorescence change has been shown to correspond to the rate of ATP cleavage. The second-order rate constant of ATP binding to MHF, $K_1 \cdot k_{+2}$ (see Table 1), was calculated from analysis of the data obtained at low ATP concentrations (Fig. 3*B*) and was half that for ATP binding to rabbit S1 ($0.94 \times 10^6\ M^{-1} s^{-1}$ compared with $1.9 \times 10^6\ M^{-1} s^{-1}$).

The binding of ADP to S1 also produces an increase in protein fluorescence and has been used to measure the rate

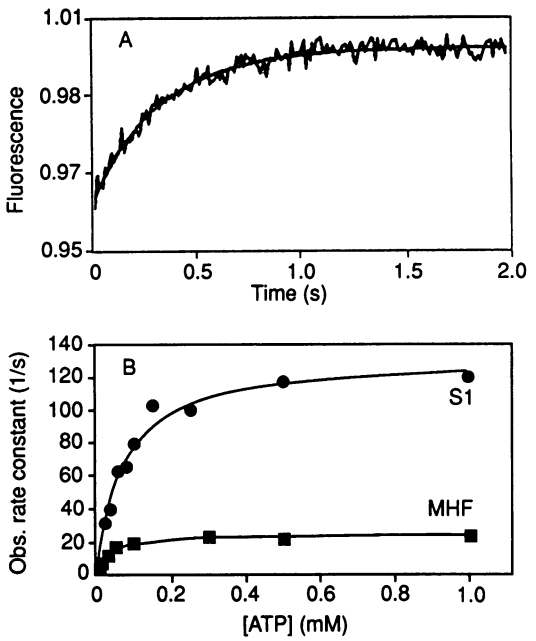

FIG. 3. Binding of ATP to rabbit S1 and *Dictyostelium* MHF at 20°C. (*A*) Stopped-flow record obtained on mixing 0.25 μM MHF with 4 μM ATP. The solid line is the best fit to a single exponential. $k_{obs} = 3.12\ s^{-1}$. (*B*) Dependence of the rate of the observed processes on ATP concentration. The data were fitted to a hyperbolic function with k_{max} values of $131\ s^{-1}$ for S1 and $24.3\ s^{-1}$ for MHF. Half-maximal values ($K_{0.5}$) of 68 μM for S1 and 25.8 μM for MHF were determined. Conditions were as described for Fig. 2.

of ADP binding. However, we could find no evidence of an increase in protein fluorescence on adding 25 μM ADP to 0.5 μM MHF. This could be due to ADP binding very weakly to MHF, or binding with no change in protein fluorescence, or both. The rate of binding of 200 μM ATP to MHF was reduced when either ATP or MHF was mixed with 25 μM ADP, suggesting that ADP does bind to MHF. This experiment did not allow an estimate of the affinity of ADP for MHF to be made. Therefore, the binding of a fluorescent analogue of ADP, mantADP, was examined.

Binding of mantADP to S1 results in an ≈2.6-fold enhancement in intrinsic *N*-methylanthraniloyl fluorescence (21). mantADP fluorescence can also be excited via energy transfer from S1 tryptophan residues (21). Similar enhancements in mantADP fluorescence (2.2-fold) and energy transfer fluorescence were observed on formation of the MHF·mantADP complex. The rate of binding of mantADP to *Dictyostelium* MHF was followed by monitoring mantADP fluorescence. At low concentrations (≤5 μM) this was excited directly at 360 nm. At higher concentrations (≥5 μM) energy transfer excited at 295 nm was observed. At 5 μM mantADP measurements were taken at both excitation wavelengths and nearly identical rates were observed. A typical transient is shown in Fig. 4*A*, while the dependence of the rate of the observed processes on mantADP concentration is plotted in Fig. 4*B*. The second-order rate constants obtained from the slope of this plot were $2.9 \times 10^6\ M^{-1}s^{-1}$ for S1 and $0.9 \times 10^6\ M^{-1}s^{-1}$ for MHF. This is equivalent to $K_1 \cdot k_{+2}$ for ATP binding, and similar values were obtained for mantATP binding ($3.2 \times 10^6\ M^{-1}s^{-1}$ and $0.7 \times 10^6\ M^{-1}s^{-1}$ for S1 and MHF, respectively).

The rate of dissociation of mantADP from MHF was measured by displacement of the nucleotide analogue from a 0.5 μM MHF·mantADP complex by 100 μM ATP. This yielded a dissociation rate constant (k_{-2}) of $1.5\ s^{-1}$, compared with a published value for rabbit S1 of $0.3\ s^{-1}$ (21). The ratio of these two measurements, $k_1 \cdot k_{+2}/k_{-2}$, gives a value of $0.6 \times 10^6\ M^{-1}$ for the equilibrium association constant of the MHF·mantADP complex. This value is an order of magnitude lower than that of the S1·mantADP complex.

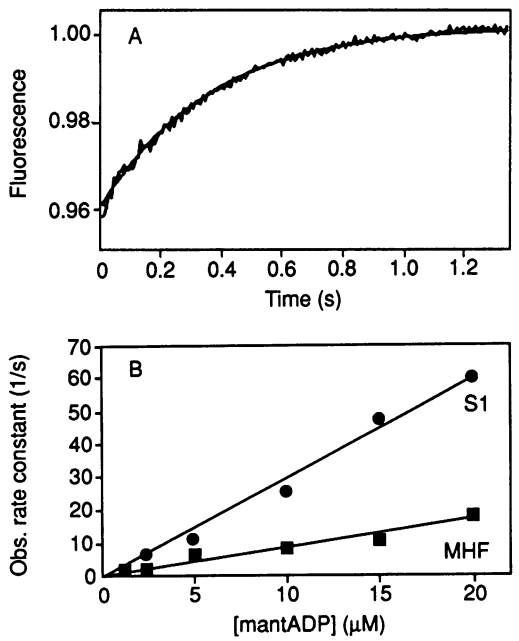

FIG. 4. Binding of mantADP to S1 and MHF. (*A*) Stopped-flow record obtained on mixing 0.25 μM MHF with 2.5 μM mantADP. The solid line is the best fit to a single exponential. $k_{obs} = 2.53\ s^{-1}$. The fluorescence of mantADP, excited at 360 nm, was observed. (*B*) Dependence of the rate of the observed processes on mantADP concentration. Second-order rate constants ($K_1 \cdot k_{+2}$) of $2.9 \times 10^6\ M^{-1}s^{-1}$ (S1) and $0.9 \times 10^6\ M^{-1}s^{-1}$ (MHF) were determined. Conditions were as described for Fig. 2.

DISCUSSION

The results presented here demonstrate that the mechanism of interaction of MHF with actin and nucleotide is essentially the same as that observed with the motor domains of conventional myosins. The affinity of MHF for actin is indistinguishable from that of rabbit myosin S1. Previous studies have shown that K_{app} (the actin concentration required for half-maximum activation of the ATPase) is similar for *Dictyostelium* heavy meromyosin and vertebrate heavy meromyosins (22). Together, these two results suggest a high degree of conservation in the actin-binding domain of myosins from species as distantly related as *Dictyostelium* and rabbit.

In contrast to their interaction with actin, *Dictyostelium* and rabbit myosins show clear differences in their interaction with nucleotides. The rate of the ATP induced dissociation of actoMHF is >10-fold slower than that observed for rabbit skeletal muscle S1. This was shown to be due to a 10-fold reduction in the rate constant of the ATP-induced isomerization of the actoMHF complex. A lower rate constant has been observed for this step for many slow vertebrate myosins and their subfragments (15, 17, 23). However, the affinity of ATP for the actoMHF complex before the isomerization is similar to that observed for other myosins at the same ionic strength (23). Likewise, the affinity of ADP for actoMHF is very close to that for actoS1. This finding, however, is unexpected, as this affinity has been shown to vary between different vertebrate myosins. Indeed, the rate of ADP dissociation from actomyosin has been suggested to be one of the principal factors defining the maximum speed of muscle shortening for a given myosin type (24).

The rate of ATP binding to MHF in the absence of actin was half that observed for S1. ATP binding is thought to be a two-step process, the formation of a fast collision complex followed by an almost irreversible conformational change. The second-order rate constant for ATP binding defines $K_1 \cdot k_{+2}$ (Table 1) and lower values of K_1, k_{+2}, or both could be responsible for the lower observed rates. The apparent second-order rate constant for ATP binding to S1 does not vary significantly across all the vertebrate skeletal myosin S1 molecules which have been studied (15). ATP is hydrolyzed in a slower step following the ATP-induced conformational change, and the rate of the hydrolysis step is measured as the maximum rate of intrinsic fluorescence change. This is significantly slower for MHF than for S1 but is similar to that of vertebrate gizzard myosin S1 (15).

Table 1. Summary of rate constants of the interaction of nucleotides with rabbit S1 and *Dictyostelium* MHF

$$M + ATP \underset{k_{-1}}{\overset{k_{+1}}{\rightleftharpoons}} M{\cdot}ATP \underset{k_{-2}}{\overset{k_{+2}}{\rightleftharpoons}} M^*{\cdot}ATP \underset{k_{-3}}{\overset{k_{+3}}{\rightleftharpoons}} M{\cdot}ADP{\cdot}P_i$$

Nucleotide	Rate constant	S1	MHF
ATP	$K_1 \cdot k_{+2}$ ($M^{-1}s^{-1}$)	1.9×10^6	0.94×10^6
	$k_{+3} + k_{-3}$ (s^{-1})	131	24
mantATP	$K_1 \cdot k_{+2}$ ($M^{-1}s^{-1}$)	3.2×10^6	0.7×10^6
mantADP	$K_1 \cdot k_{+2}$ ($M^{-1}s^{-1}$)	2.9×10^6	0.9×10^6
	k_{-2} (s^{-1})	0.3	1.5
	$K_1 \cdot k_{+2}/k_{-2}$ (M^{-1})	10×10^6	0.6×10^6

$K_1 \cdot k_{+2}$ = observed second-order rate constant of nucleotide binding to S1 or MHF, where the observed rate constant was proportional to nucleotide concentration. $k_{+3} + k_{-3}$ = limiting rate constant of protein fluorescence signal at high concentrations of nucleotide. k_{-2} = observed first-order rate constant of the displacement of mantADP from the complex.

DISCUSSION

In the case of rabbit S1, a protein fluorescence change is thought to occur on both the conformational change following ATP binding and the subsequent hydrolysis step (19, 20). The key indication of this is that the observed amplitude of the fluorescence change decreases at high ATP concentrations. For MHF the observed fluorescence amplitude is approximately half that for S1, and no loss of amplitude is observed at high ATP concentrations. This is consistent with a fluorescence change occurring only on the hydrolysis step. This interpretation is supported by the results with ADP that show no increase in protein fluorescence on addition of 25 μM ADP to MHF. However, the presence of ADP does inhibit the binding of ATP to MHF, suggesting that ADP binds to the nucleotide site on MHF but does so with no increase in protein fluorescence.

The binding of mantADP to MHF produces a change in both *N*-methylanthraniloyl fluorescence and energy transfer fluorescence. The enhancement of *N*-methylanthraniloyl fluorescence is only slightly smaller than that observed with S1. mantADP binds to S1 with a 10-fold higher affinity than ADP. The rate of association is identical to that of ADP (2–3 $\times$ 10^6 $M^{-1}\cdot s^{-1}$; ref. 21), but the dissociation rate constant is 10-fold slower. We have shown that the second-order rate constant of association of mantADP with MHF is 3-fold slower than that with S1, while the rate of dissociation is 5-fold higher than from S1. The ratio of rate constants gives an affinity of mantADP for MHF of 0.6 $\times$ 10^6 M^{-1}, compared with 10 $\times$ 10^6 for S1.

The data on ADP binding to MHF are consistent with the affinity being of the order of 10 times weaker than that for rabbit S1, suggesting an association constant of less than 5 $\times$ 10^4 M^{-1}. An association constant of this size is difficult to measure given the limited amount of MHF available, especially as there is no readily observable signal. However, thermodynamic consistency can be checked by measuring the remaining association constants in the following scheme:

$$\begin{array}{ccc} A + M + D & \overset{K_A}{\rightleftharpoons} & A\cdot M + D \\ {\scriptstyle K_D}\uparrow\downarrow & & \uparrow\downarrow{\scriptstyle K_{AD}} \\ A + M\cdot D & \underset{K_{DA}}{\rightleftharpoons} & A\cdot M\cdot D \end{array}$$

Scheme III

where $K_D = K_A \cdot K_{AD}/K_{DA} = 2.7 \times 10^4\ M^{-1}$ (Table 2). Thus, a much weaker binding of ADP to MHF is consistent with all the data we have collected. ADP therefore binds to actoMHF with a similar affinity as to actoS1, but binds more weakly to MHF alone than to S1, and so is less able to dissociate actin from MHF.

Table 2. Summary of rate constants of the interaction of nucleotides with actoS1 and actoMHF

$$\begin{array}{c} \qquad\qquad ATP \\ A + M \overset{K_A}{\rightleftharpoons} A\cdot M \overset{K_a}{\rightleftharpoons} A\cdot M\cdot ATP \overset{k_b}{\rightarrow} A + M\cdot ATP \\ A + M + ADP \overset{K_D}{\rightleftharpoons} A + M\cdot ADP \overset{K_{DA}}{\rightleftharpoons} A\cdot M\cdot ADP \overset{K_{AD}}{\rightleftharpoons} A\cdot M + ADP \end{array}$$

Rate constant	ActoS1	ActoMHF
K_A (M^{-1})	14 $\times$ 10^6	14 $\times$ 10^6
K_a (M^{-1})	500*	320
k_b (s^{-1})	5000*	450
K_D† (M^{-1})	1.2 $\times$ 10^5	2.7 $\times$ 10^4
K_{DA} (M^{-1})	1 $\times$ 10^6	5 $\times$ 10^6
K_{AD} (M^{-1})	8.6 $\times$ 10^3	10.6 $\times$ 10^3

*As predicted by Millar and Geeves (16).
†Calculated as the product $K_A \cdot K_{AD}/K_{DA}$.

The data presented here demonstrate that MHF is capable of making the same interaction with actin as rabbit skeletal myosin S1, but the binding of both ATP and ADP is altered. ATP is shown to induce a slower conformational change in both MHF and actoMHF. For actoS1, the nucleotide-induced conformational change has been proposed to be closely coupled to the force-generating transition of the crossbridge cycle. The observation that ATP produces a slower transition with both MHF and actoMHF, and that ADP is not able to induce the transition at all, suggests a different degree of coupling between the nucleotide and actin binding sites on MHF. While the functional significance of these differences is not clear, it will be interesting to learn whether this is a common feature of nonmuscle myosins.

In this study, we have demonstrated the viability of the recombinant approach to the isolation of a functional motor protein in sufficient quantities to carry out a complete and detailed kinetic characterization of its enzymatic activities. This approach can be extended to the generation of specifically modified myosin motor domains to allow fine mapping of functional regions and can be used to link structural features to the motor activity of myosins.

We thank Mr. E. Nerou for excellent technical assistance. This work was supported by the Medical Research Council and the Wellcome Trust. M.A.G. is a Royal Society University Research Fellow.

1. Taylor, E. W. (1979) *Crit. Rev. Biochem.* **6**, 103–164.
2. Geeves, M. A., Goody, R. S. & Gutfreund, H. (1984) *J. Musc. Res. Cell Motility* **5**, 351–361.
3. Manstein, D. J., Ruppel, K. M. & Spudich, J. A. (1989) *Science* **246**, 656–658.
4. Toyoshima, Y. Y., Kron, S. J., McNally, E. M., Niebling, K. R., Toyoshima, C. & Spudich, J. A. (1987) *Nature (London)* **328**, 536–538.
5. Kubalek, E. W., Uyeda, T. Q. P. & Spudich, J. A. (1993) *Mol. Biol. Cell* **3**, 1455–1462.
6. Margossian, S. S. & Lowey, S. (1982) *Methods Enzymol.* **85**, 55–71.
7. Weeds, A. G. & Taylor, E. W. (1975) *Nature (London)* **257**, 54–56.
8. Lehrer, S. S. & Kewar, G. (1972) *Biochemistry* **11**, 1211–1217.
9. Criddle, A. H., Geeves, M. A. & Jeffries, T. (1985) *Biochem. J.* **232**, 343–349.
10. West, J. J., Nagy, B. & Gergely, J. (1967) *Biochem. Biophys. Res. Commun.* **29**, 611–629.
11. Hiratsuka, T. (1983) *Biochim. Biophys. Acta* **742**, 496–508.
12. Kouyama, T. & Mihashi, K. (1981) *Eur. J. Biochem.* **114**, 33–38.
13. Geeves, M. A. & Jeffries, T. A. (1988) *Biochem. J.* **256**, 41–46.
14. Eccleston, J. F., Geeves, M. A., Trentham, D. R., Bagshaw, C. R. & Mrwa, U. (1975) in the *26th Colloquium Gesellschaft für Biologische Chemie*, eds. Heilmayer, L. M. G., Ruegg, J. C. & Wieland, T. (Springer, Berlin), pp. 15–21.
15. Marston, S. B. & Taylor, E. W. (1980) *J. Mol. Biol.* **139**, 573–600.
16. Millar, N. C. & Geeves, M. A. (1983) *FEBS Lett.* **160**, 141–148.
17. Siemankowski, R. F. & White, H. D. (1984) *J. Biol. Chem.* **259**, 5045–5053.
18. Bagshaw, C. R. & Trentham, D. R. (1974) *Biochem. J.* **141**, 331–349.
19. Johnson, K. A. & Taylor, E. W. (1978) *Biochemistry* **17**, 3432–3442.
20. Millar, N. C. & Geeves, M. A. (1988) *Biochem. J.* **249**, 735–743.
21. Woodward, S. K. A., Eccleston, J. F. & Geeves, M. A. (1991) *Biochemistry* **30**, 422–430.
22. Troung, T., Medley, Q. C. & Côté, G. P. (1992) *J. Biol. Chem.* **14**, 9767–9772.
23. Marston, S. B. (1992) in *Biochemistry of Smooth Muscle*, ed. Stevens, N. L. (CRC, Boca Raton, FL), Vol. 1, pp. 167–191.
24. Siemankowski, R. F., Wiseman, M. O. & White, H. D. (1985) *Proc. Natl. Acad. Sci. USA* **82**, 658–662.